

# An ultra-compact hairpin band pass filter with additional zero points

Ma, Kaixue; Yeo, Kiat Seng; Ma, Jianguo; Do, Manh Anh

2007

Ma, K., Yeo, K. S., Ma, J. G., & Do, M. A. (2007). An ultra-compact hairpin band pass filter with additional zero points. *IEEE Microwave and Wireless Components Letters*, 17(4), 262-264.

<https://hdl.handle.net/10356/91738>

<https://doi.org/10.1109/LMWC.2007.892955>

---

© 2007 IEEE. Personal use of this material is permitted. However, permission to reprint/republish this material for advertising or promotional purposes or for creating new collective works for resale or redistribution to servers or lists, or to reuse any copyrighted component of this work in other works must be obtained from the IEEE. This material is presented to ensure timely dissemination of scholarly and technical work. Copyright and all rights therein are retained by authors or by other copyright holders. All persons copying this information are expected to adhere to the terms and constraints invoked by each author's copyright. In most cases, these works may not be reposted without the explicit permission of the copyright holder. <http://www.ieee.org/portal/site>.

*Downloaded on 20 Mar 2024 17:22:53 SGT*

# An Ultra-Compact Hairpin Band Pass Filter with Additional Zero Points

Kaixue Ma, *Member, IEEE*, Kiat Seng Yeo, Jianguo Ma, *Senior Member, IEEE*,  
and Manh Anh Do, *Senior Member, IEEE*

**Abstract** — A novel quasi-hairpin filter is presented in this letter. The generation of zero points is investigated. Second-order and fourth-order filters, based on separate coupling paths, have been implemented. The filters show ultra-compact size, steep selectivity and deep stopband with additional transmission zero points. The measured fourth-order filter operating at 1.69 GHz, with a fractional bandwidth of 10% has only an active area of  $5.5 \text{ mm} \times 6.2 \text{ mm}$  ( $0.031\lambda_0 \times 0.035\lambda_0$ ).

**Index Terms**—Zero Point, Band Pass Filter, Quasi-hairpin filter, separate coupling paths

## I. INTRODUCTION

WITH the expanding applications of mobile radio communication, compact size and low cost of passive filters become very important for miniaturized communication systems. Many publications in the literature have reported on size reduction of the filter [1]-[8]. A quarter-wavelength resonator [5],[6] has a smaller size as compared to the traditional half-wavelength resonator. The spiral resonators have emerged as one of the most compact resonators [1], [2],[3]. Although the spiral resonator with two open ends is investigated extensively, little work has been reported in designing a spiral-like resonator with open-ground ends. In this letter, spiral-like resonators with open-ground ends are used to design compact filter with good skirt selectivity. The generation mechanism of the zero points is also investigated by using a proposed method.

An ultra-compact microstrip common via band pass filter with spiral-like resonators, as shown in Fig.1 a), is introduced. It consists of two open-ground spiral-like resonators, which can be approximately treated as two folded quarter-wave length resonators. The ground via, which is shared by two resonators, provides grounding connections for two spiral-like resonators and generates the required inter-stage magnetic coupling for the filter simultaneously. The proposed filter has similar filter topology as in [8]. However, the analysis in [8] can not analyze this filter with spiral-like resonator with acceptable accuracy.

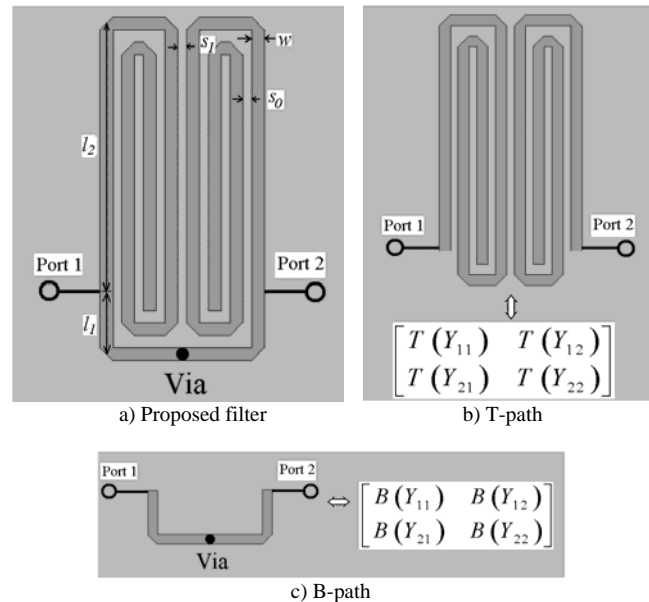


Fig.1. Proposed second-order filter configuration and the equivalent circuits

Practically, characterizing the whole structure with two coupling paths by using full-wave EM software can only see the combination effects. It is difficult to see the operating mechanism behind the two coupling paths. Actually, the filter in Fig.1 a) can be equivalent to an electric coupling part (T-path) in Fig.1 b) and a magnetic coupling part (B-path) in Fig.1 c), if the weak electromagnetic coupling between the T-path and the B-path is neglected. By investigating the T-path and B-path separately, the characteristics of the filter response and zero points can be predicted with acceptable accuracy. Based on the investigation, the proposed second-order and fourth-order filters with good selectivity, additional zero points and much compact size are designed and implemented.

## II. SECOND ORDER FILTER REALIZATION

In order to investigate the characteristics of the filter in Fig.1 a), the equivalent T-path and B-path are investigated separately. The structures in the T-path are two coupled open end spirals. The characteristics of the T-path in Fig.1 b) and B-path in Fig.1 c) can be investigated by using the full-wave EM software HFSS. Since the structures are symmetrical, the calculated S-parameter can be transferred to Y-parameter using following equations:

Manuscript received August 18, 2006.

K. Ma is currently with MEDS Technologies Pte. Ltd, Singapore, 569876 email: [kxma@ieee.org](mailto:kxma@ieee.org)

K. S. Yeo and M. A. Do are with Center for Integrated Circuits & Systems (CICS), Nanyang Technological University (NTU), Singapore 639798.

J.-G. Ma is with University of Electronic Science and Technology of China (UESTC), Chengdu, P. R. China.

$$B/T(Y_{21}) = B/T(Y_{12}) = Y_0 \frac{-2B/T(S_{21})}{(1 - B/T(S_{11}))^2 - B/T(S_{21})^2} \quad (1)$$

$$B/T(Y_{11}) = B/T(Y_{22}) = Y_0 \frac{1 - B/T(S_{11})^2 + B/T(S_{21})^2}{(1 + B/T(S_{11}))^2 - B/T(S_{21})^2} \quad (2)$$

where  $Y_0$  is the terminal admittance. From equations (1) and (2), the Y-matrix for T-path in Fig.1 b) and B-path in Fig.1 c) can be calculated separately respectively. The characteristics of the filter in Fig.1 a) can be investigated by using the derived Y-parameters. The total Y-matrix can be calculated by summing of the Y-matrices of the T-path and B-path. The total Y-matrix is used to calculate the S-matrix of structure in Fig.1 a) as given in equations (3) and (4).

$$S_{21} = \frac{-2[T(Y_{21}) + B(Y_{21})]Y_0}{[Y_0 + T(Y_{11}) + B(Y_{11})]^2 - [T(Y_{21}) + B(Y_{21})]^2} \quad (3)$$

$$S_{11} = \frac{Y_0^2 - [T(Y_{11}) + B(Y_{11})]^2 + [T(Y_{21}) + B(Y_{21})]^2}{[Y_0 + T(Y_{11}) + B(Y_{11})]^2 - [T(Y_{21}) + B(Y_{21})]^2} \quad (4)$$

The RT/Duroid 6010 substrate with relative permittivity of  $\epsilon_r = 10.2$  and thickness of 0.635 mm are used in the following analysis and design. The calculated results for two different cases (case 1 and case 2) are shown in Fig.2 and Fig.3. Under lossless or low loss condition, the generation of the zero points of the filter in Fig.1 a) should satisfy the condition of equation (5) as the two cases are compared in Fig.2.

$$\text{imag}(Y_{21}) = \text{imag}(T(Y_{21}) + B(Y_{21})) = 0 \quad (5)$$

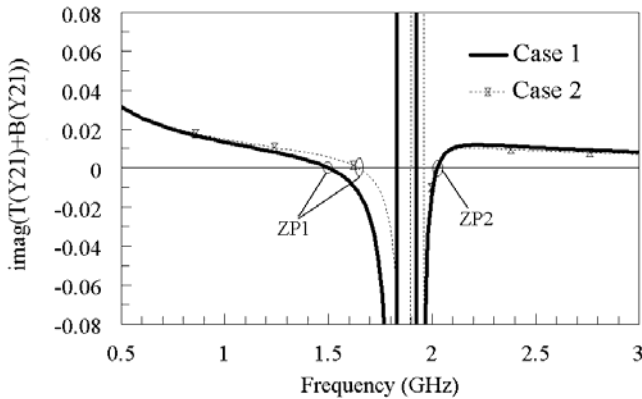


Fig.2. The impedance and zero points of the filter in Fig.1 a). Filter dimensions:  $l_1=1.0$  mm,  $l_2=4.3$  mm,  $w=0.2$  mm,  $s_0=0.15$  mm, radius of via  $R_{\text{via}}=0.1$  mm,  $s_l=0.15$  mm for case 1,  $s_l=0.35$  mm for case 2

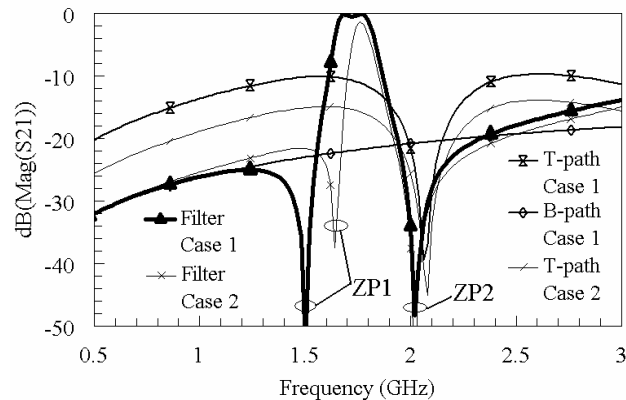


Fig.3. The transmission characteristics of the filter in Fig.1 a).

The calculated first zero points ZP1 for two cases are 1.5GHz and 1.64 GHz respectively. The second zero points ZP2 for two cases are almost at the same frequency point of 2.03GHz. The locations of the analyzed zero points, shown in Fig.2, agree well with that in the Fig.3. The coupling characteristics of the T-path, B-path and the filter are illustrated in Fig.3. It can be seen that at low operating frequency range below ZP1, the inter-stage coupling is mainly determined by the magnetic coupling in B-path, while at high frequency range above ZP2, the inter-stage coupling is determined by both electric coupling in T-path and the magnetic coupling in B-path. In the frequency range below ZP1, the electric coupling in T-path is much larger than the magnetic coupling in B-path as well as total inter-stage coupling of the filter. Comparing cases 1 and 2, it is interesting to note that the only difference is  $s_l$  in T-path. This is because that  $s_l$  determines the electric coupling coefficient and the coupling in the passband of the filter is dominant by the electric coupling. As illustrated in case 1, the reduced electric coupling due to the larger  $s_l$  actually reduces the total coupling especially in passband and thus reduces the bandwidth of the filter. The generation of the ZP1 is due to the canceling effect of the electric coupling and magnetic coupling. The ZP2 is due to the self-resonance of the open end spiral in the T-path. This is because at self-resonant frequency, the open end spiral behaves as a bandstop resonator with zero input impedance. In Fig.4, the simulated results by using equations (3) and (4) of the proposed filter are compared with the measured results. Good agreement between the two results is achieved. The frequency shift of 4.8% between the simulation and the measurement for the spiral-like resonators is acceptable. The measured insertion loss of the filter is 2dB, and the filter size is only 5.5 mm by 2.7 mm (the I/O port connection lines are not included).

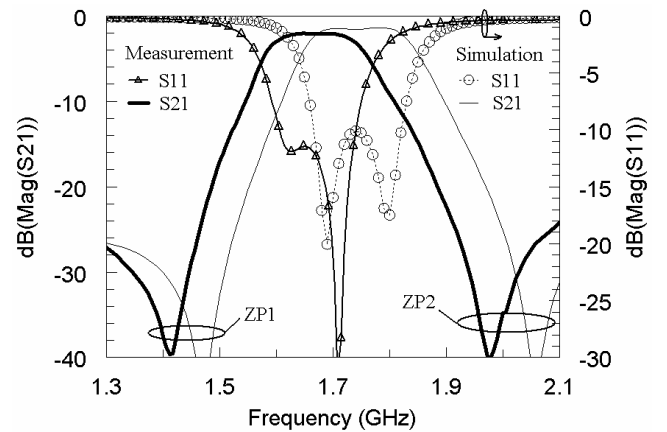


Fig.4. Comparison of measured and simulated results of proposed second-order hairpin filter

### III. FOURTH ORDER FILTER REALIZATION

The configuration and the topology of a fourth-order band pass filter are shown in Fig.5 a) and b) respectively. The two separate coupling paths with dominant electric couplings are introduced between resonators 1 and 2 as well as between 3 and 4. The external quality factor  $Q_e$  and the inter-stage coupling coefficients can be calculated from [5][6]. The optimized dimensions of the filter are:  $l_1=1.0$  mm,  $l_2=4.3$  mm,  $l_3=1.5$  mm,

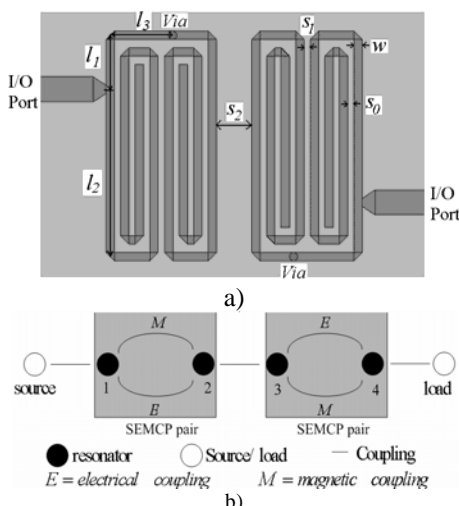


Fig. 5 Proposed fourth-order hairpin filter configuration and the topology a) Filter configuration b) Filter topology

$w=0.2$  mm,  $s_0=0.15$  mm,  $s_1=0.15$  mm,  $R_{via}=0.1$  mm,  $S_2=0.85$  mm. In Fig.6, the simulated results and the measured results in the frequency range of 1.0 GHz~2.5 GHz are compared. The

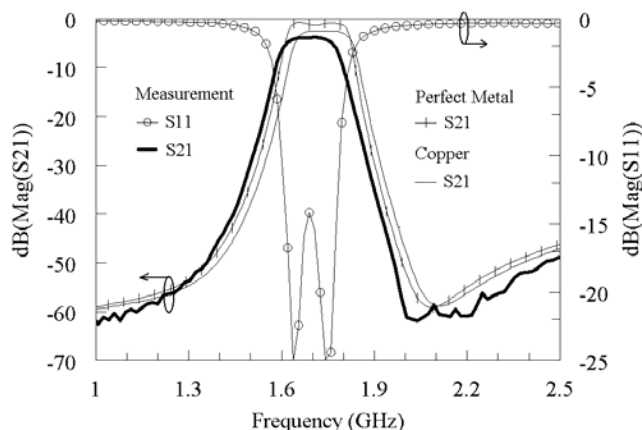


Fig.6. Comparison of measured and simulated results of proposed fourth-order quasi-hairpin filter.

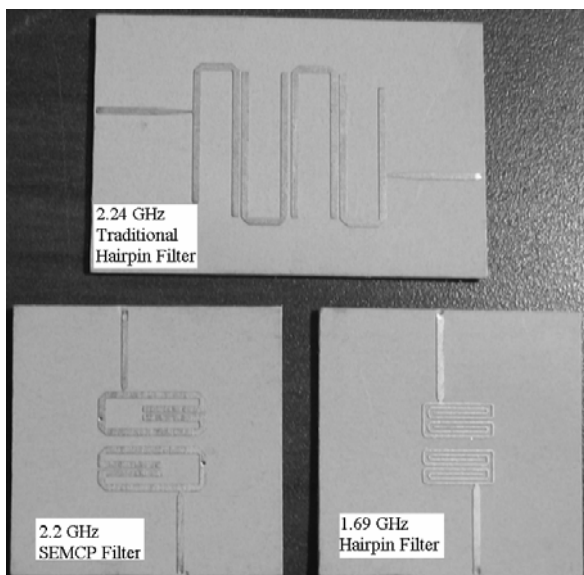


Fig.7. Photos of a 2.24 GHz traditional hairpin filter, a 2.2 GHz SEMCP filter and a 1.69GHz proposed hairpin filter.

simulated results agree well with the simulated results. The results of the filter show deep stopband rejection and good skirt selectivity. The filter characteristics with perfect conductor and copper conductor are also compared. The minimum insertion loss of the filter with a perfect conductor is 0.8 dB, and the minimum insertion loss of the filter with copper conductor is 2.5 dB. The filter with a copper conductor has a narrower bandwidth than the filter with a perfect conductor. The measured fourth-order filter operates at 1.69 GHz, has a fractional bandwidth of 10% and an insertion loss of 3.2 dB. The rejections at 2 GHz and at 1.27 GHz are 61.2 dB and 55 dB respectively. The photos of a traditional hairpin filter, a SEMCP filter [8] and the proposed hairpin filter are illustrated in Fig.7. The size of the proposed fourth-order hairpin filter occupies an area as small as  $5.5 \text{ mm} \times 6.2 \text{ mm}$  ( $0.031\lambda_0 \times 0.035\lambda_0$ ). The size of the proposed hairpin filter is much smaller than that of the traditional fourth-order hairpin filter ( $0.094\lambda_0 \times 0.11\lambda_0$ ) and the SEMCP filter ( $0.06\lambda_0 \times 0.0545\lambda_0$ ) in [8] ( $\lambda_0$  is the free space wavelength at operating frequency).

#### IV. CONCLUSION

In this paper, a novel hairpin filter based on separate coupling paths is proposed and implemented. Second-order and fourth-order hairpin filters with good skirt selectivity and compact size are implemented on standard planar print circuit board. The zero point generation, the coupling characteristics and the conductor loss of the proposed filter are investigated. The proposed compact hairpin filter configuration should be useful for miniaturized filter implementation.

#### ACKNOWLEDGMENT

The authors would like to thank K.T. Chan from MEDs company for helping in the fabrication.

#### REFERENCES

- [1] S.B.Cohn, "Parallel-coupled transmission-line resonator filters," *IRE Trans. Microwave Theory Tech.*, vol.6, pp.223-231, Apr. 1958
- [2] E. G. Cristal and S. Frankel, "Hairpin-line and hybrid hairpin-line half-wave parallel-coupled-line filters," *IEEE Trans. Microwave Theory Tech.* vol. 20, pp. 719-728, Nov. 1972.
- [3] M. Sagawa, K. Takahashi and M. Makimoto, "Miniaturized hairpin resonator filters and their application to receiver front-end MIC's," *IEEE Trans. Microwave Theory Tech.* vol. 37, pp. 1991-1996, Dec. 1989
- [4] I. Wolff, "Microstrip bandpass filter using degenerate modes of microstrip ring resonator," *Electron. Lett.*, vol. 8, no. 12, pp.779-781, Jun. 1972
- [5] J.-S. Hong and M. J. Lancaster, *Microstrip Filters for RF/Microwave Applications*, John Wiley & Sons, Inc. 2001
- [6] G. L. Matthaei, L. Young and E.M.T. Jones *Microwave Filters, Impedance-matching Networks, and Coupling Structures*, Artech House, Dedham, MA 1964.
- [7] T. Kitamura, Y. Horii, M. Geshiro and S. Sawa, "A dual-plane comb-line filter having plural attenuation poles," *IEEE Tran. Microwave Theory Tech.* Vol.50, pp.1216-1219, April. 2004
- [8] K. Ma, J.-G. Ma, and K. S. Yeo, and M. A. Do, "A compact size coupling controllable filter with separated electric and magnetic coupling paths" *IEEE Trans. Microwave Theory Tech.*, vol.54, no.3, pp.1113-1119, Mar., 2006